Scanning Tunneling Spectroscopy of Insulating Self-Assembled Monolayers on Au(111)

André P. Labonté,[†] Steven L. Tripp,[‡] Ronald Reifenberger,*[,†] and Alexander Wei*[,‡]

Department of Physics, Purdue University, West Lafayette, Indiana 47907-1396, and Department of Chemistry, Purdue University, West Lafayette, Indiana 47907-1393

Received: February 8, 2002; In Final Form: June 3, 2002

Self-assembled monolayers (SAMs) of dodecanethiol (DDT), octadecanethiol (ODT), and resorcinarene C10 tetrasulfide (RC10TS) on Au(111) were characterized by scanning tunneling spectroscopy (STS) under ultrahigh vacuum conditions and evaluated as ultrathin resists. A voltage division factor η was used to parametrize the equilibrium Fermi energy level E_f in terms of an applied voltage bias. Nominally symmetric tunneling ($\eta \sim 0.5$) conditions were established by acquiring conductance spectra over a range of set point voltages. The electrical conductivity of the monolayers was observed to be dependent on both the monolayer thickness and the nature of the Au/S bonding. Leakage current densities across DDT and RC10TS SAMs on Au were estimated, with the latter comparing favorably with a 1.5-nm layer of SiO_2 on Si.

Introduction

Self-assembled monolayers (SAMs) of organic compounds on surfaces are ubiquitous in the design of electronic devices with molecular and nanoscale dimensions.[1−6] A key quality of many SAMs is their intrinsically low electrical conductance, a passive but essential feature for the realization of nanoscale electronics. Inadequate insulation is presently considered to be a serious hindrance to the continued miniaturization of integrated circuits; for example, quantum mechanical electron tunneling becomes the dominant source of leakage current across metal−oxide junctions as gate oxide thickness drops below 5 nm. For silicon dioxide (SiO_2), recent studies indicate that the leakage current will increase by almost 12 orders of magnitude as the thickness changes from 3.5 to 1.5 nm.[7] Quantum-mechanical calculations suggest a minimum SiO_2 thickness of 1.5−2.0 nm for chip standby power requirements,[8] although a more optimistic estimate of 1.2 nm has been suggested on the basis of the fundamental physical limits of SiO_2 as a gate dielectric.[9] At this length scale variations in oxide thickness by as little as one atomic layer on a Si wafer could result in drastic variations in device performance, making it very difficult to maintain device tolerances.

Organic SAMs are intriguing alternatives to SiO_2 as electrically insulating materials. Well-ordered SAMs are uniform in thickness and can be designed with tunable interfacial properties, providing unique processing advantages for device fabrication. The electrical properties of SAMs have obvious ramifications for nanostructured device engineering; for example, SAMs composed of bifunctional molecules have enabled the layered deposition of conductive or semiconductive nanoparticulate films.[10] Electron-transfer rates across SAMs on Au(111) surfaces have been studied by electrochemical methods[11−14] and conducting-probe force microscopy[15,16] and have been correlated with changes in chain length and the molecular composition of the SAM.

Scanning tunneling microscopy (STM) can probe molecular periodicities[17−25] and electronic states at the molecular level[26−32] of SAMs. Ideally, one would like to place the STM probe tip directly over a molecule within a SAM and measure its conductance as a function of applied voltage (V_{bias}), but direct measurements of this type are often frustrated by difficulties in the precise determination of the tip-molecule separation. If the tip−molecule separation results in a vacuum gap of unknown width, or if the tip exerts sufficient force to deform the monolayer, an inaccurate measurement of the conductance may result.[15] Earlier STM studies of SAMs on Au(111) have investigated the relationship of the tunneling current to the tip−sample separation in detail and support a double-layer tunnel junction model in which the conductance is a product of the transmission across the SAM and the vacuum gap.[31,33] The transmissions are exponentially dependent on the thickness of their respective media, but their accurate measurement requires exact knowledge of the distance between tip and sample, as well as a well-defined physical model of the SAM for a valid estimation of decay constants.

Here we describe a systematic method for characterizing the tunnel barrier across highly insulating SAMs on Au(111), using scanning tunneling spectroscopy (STS) techniques under ultrahigh vacuum (UHV) conditions. Previous STS studies have been used in conjunction with theoretical developments pioneered by Datta to estimate the transport properties of moderately conductive organic "wires" as a function of molecular structure and chemical bonding.[10,26,28−30,32,34] Such treatments can in principle be extended to more insulating molecules, but the low tunneling currents at zero bias (often less than 1 pA) are accompanied by substantial experimental error. To this end, we have determined that the systematic evaluation of conductance at a threshold voltage bias enables us to estimate the conductivity of the molecules comprising the SAM to the first degree of approximation, which can then be interpreted in terms of molecular structure. We have applied this method toward measuring the electrical conductances of SAMs prepared from dodecanethiol (DDT), octadecanethiol (ODT), and resorcinarene C10 tetrasulfide (RC10TS) on Au(111) (see Figure 1). The structure and electrochemically insulative properties of these well-ordered monolayers have been characterized by a number of experimental methods including STM,[17−25,27,35] and their

[†] Department of Physics.
[‡] Department of Chemistry.

10.1021/jp025626l CCC: $22.00
Published on Web 08/02/2002

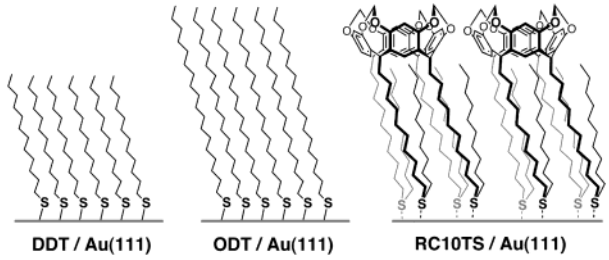

Figure 1. Self-assembled monolayers (SAMs) of dodecanethiol (DDT), octadecanethiol (ODT), and resorcinarene C10 tetrasulfide (RC10TS) adsorbed on Au(111) (only a few molecules are presented for clarity).The estimated thicknesses of the DDT, ODT, and RC10TS SAMs are 1.4, 2.0, and 2.0 nm, respectively.[12,45,44]

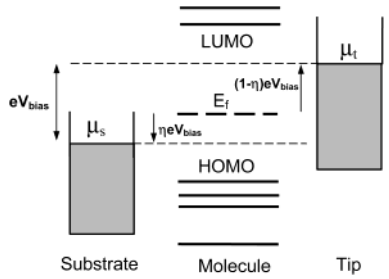

Figure 2. Energy diagram for STS experiment showing the positions of μ_t and μ_s relative to the equilibrium Fermi energy, E_f.[28−30,32] The voltage division factor, η, affects the limits of integration in eq 1.

differences in thickness or chemical bonding to Au make them ideal substrates for evaluating this approach.

Theoretical Considerations

Using the Landauer−Buttiker formalism, the current−voltage $I-V$ relationship can be calculated if the transmission probability $T(E,V)$ of an electron through a molecule is known as a function of applied voltage bias:

$$I = \frac{2e}{h}\int_{-\infty}^{\infty} \mathrm{d}E\, T(E,V)[f(E-\mu_t) - f(E-\mu_s)] \qquad (1)$$

Here E is the electron energy, μ_t and μ_s are the Fermi energy levels of the tip and the substrate, respectively (see Figure 2), and $f(E)$ is the Fermi−Dirac distribution function. At room temperature, the cutoff in the Fermi−Dirac function effectively restricts the limits of the integral to μ_t and μ_s. In the limit of low bias voltage, $\mu_t - \mu_s = eV_{bias}$, so that eq 1 can be expressed as

$$I = \frac{2e^2}{h}T(E_f)V_{bias} = G_o T(E_f)V_{bias} \qquad (2)$$

This simplified form describes $T(E_f)$ as a direct function of current flow, scaled by the quantum of conductance G_o. Calculations based on this formalism have been widely used to describe the molecular conductance of a number of organic structures based on their conductance spectra.[28,29,32,34,36−40] It is important to note that molecules with similar chemical structures can give rise to completely different conductances if the transmission function is modulated by extrinsic factors such as differences in chemical bonding at the substrate−molecule interface, as has been predicted theoretically.[37,41]

Three factors are critical in determining molecular conductance: $T(E,V)$ itself, which in principle can be derived from the energy levels of a molecule adsorbed onto the substrate, the alignment of the chemical potentials μ_t and μ_s with respect to the molecular energy levels, and knowledge of the spatial variation of the electrostatic potential. In large metallic structures, the electrostatic potential tracks very well with the chemical potential. However, this is not necessarily the case in structures with molecular scale dimensions, in which differences between the local value of the electrostatic potential and chemical potential are usually unknown. These issues are addressed by defining a voltage division factor η to parametrize the position of μ_t and μ_s relative to the equilibrium Fermi energy level E_f in terms of the applied voltage V_{bias}:[28−30,32]

$$\mu_s = E_f - \eta eV_{bias} \qquad (3)$$

$$\mu_t = E_f + (1-\eta)eV_{bias} \qquad (4)$$

Based upon eqs 3 and 4, the $I-V$ response can be expected to be reasonably symmetric when η is close to 0.5. Establishing conditions for $\eta \sim 0.5$ across a given SAM obviates the need to obtain precise tip−sample distances or monolayer thicknesses and provides a systematic and practical approach for measuring electrical conductances across highly insulating SAMs.

Experimental Section

DDT and ODT were obtained from Aldrich and used without further purification. RC10TS was prepared according to literature procedures.[42] Micron-sized domains of atomically flat Au(111) were prepared from commercial gold films evaporated onto a Cr-backed borosilicate glass substrate (Metallhandel Schroer GmbH) by heat treatment with a propane flame. Substrates were rinsed sequentially in deionized water and ethanol and then soaked overnight in 1 mM ethanolic solutions of DDT, ODT, or RC10TS.[12,43,44] SAMs were characterized by reflective-absorption infrared spectroscopy (RAIRS) and optical ellipsometry and were found to be consistent with values reported in the literature.[44−46] Freshly prepared SAMs were transferred in a UHV insertion chamber operating at a pressure of 5×10^{-9} Torr. STS studies were performed on a home-built STM housed in a stainless steel vacuum chamber operating under UHV conditions at pressures below 2×10^{-9} Torr. Images of the underlying Au grain structure could routinely be achieved with monolayers of DDT, but imaging the Au substrate through monolayers of ODT and RC10TS proved more difficult and were characterized by occasional tip switching that would occur randomly in the image.

STS measurements were conducted using mechanically cut Pt/Ir tips and were repeated with two different tips to ensure reproducibility and to minimize possible artifacts. Set voltages corresponding to $\eta \sim 0.5$ conditions were established by lowering an initially high set voltage bias (V_{set}) in 0.5 V decrements while a constant tunneling current of 0.2 nA was maintained using computer-controlled proportional-integral-differential (PID) feedback. Set point voltages below a threshold value V_{min} produced topographic images with high levels of noise, indicating that the tip was buried in the SAM. $I-V$ curves were obtained by shutting off the feedback loop and recording the tunneling current as a function of voltage between $\pm V_{set}$ for different set point voltages. $I-V$ measurements were averaged over 40 scans per set point voltage for a total sampling time of 2 s and repeated at several locations across the SAM to ensure reproducibility. The standard error for the set point current was approximately 10%. First-order derivatives ($\mathrm{d}I/\mathrm{d}V$) were obtained by performing point-to-point sliding averages of the $I-V$ data.

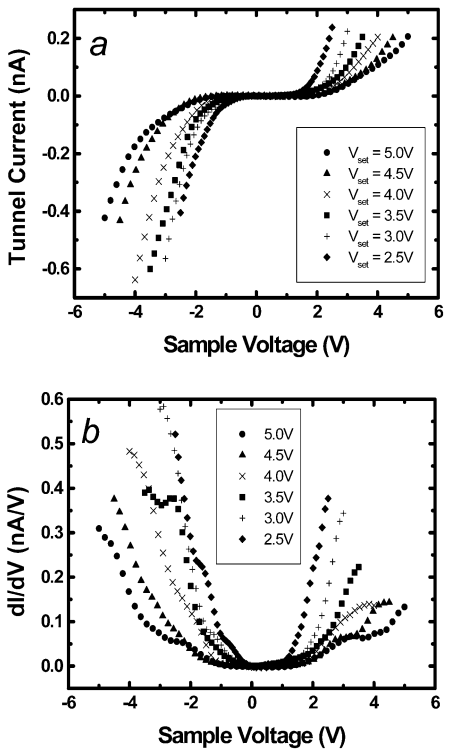

Figure 3. (a) $I-V$ data for DDT for a series of set voltages and a set current of 0.2 nA. (*b*) dI/dV data for DDT for a series of positive set voltages and a set current of 0.2 nA. The most symmetric dI/dV data are observed at a set voltage of 2.5 ± 0.2 V.

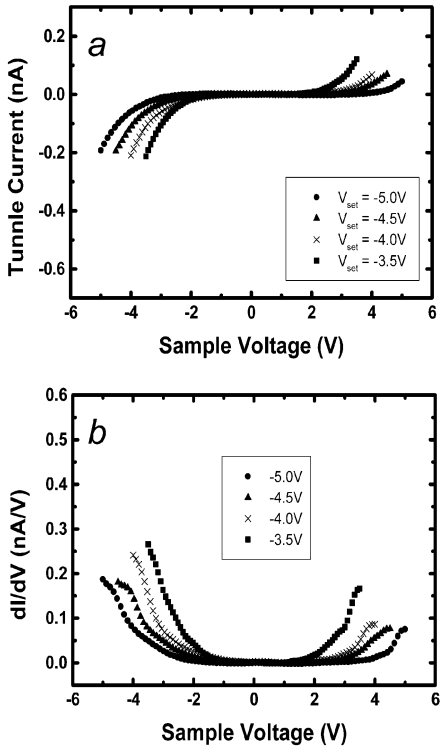

Figure 4. (a) $I-V$ data for ODT for a series of set voltages and a set current of 0.2 nA. (b) dI/dV data for ODT for a series of negative set voltages and a set current of 0.2 nA. The most symmetric dI/dV data are observed at a set voltage of -3.5 ± 0.2 V.

Results and Discussion

The value of η is close to 0.5 when the electrostatic coupling between the tip and molecule is comparable to the coupling between the molecule and substrate. Conditions corresponding to $\eta \sim 0.5$ were achieved at a threshold set voltage V_{min} demarcating the transition between stable and unstable feedback, the latter characterized by high levels of noise in both the *z*-piezo feedback voltage and tunnel current (see Experimental section).[47] For a tunnel current of 0.2 nA, this transition occurs at a V_{min} of $+2.5 \pm 0.2$ V for DDT, -3.5 ± 0.2 V for ODT, and -4.0 ± 0.2 V for RC10TS. The polarity for these values of V_{min} reflects the somewhat arbitrary choice of the sample voltage used during the initial STM imaging of the substrates, and does not affect data interpretation.

The $I-V$ data becomes more symmetric as the set voltage approaches V_{min}. $I-V$ data acquired as a function of V_{set} should become increasingly symmetric about the origin after each decrement, indicating the onset of the $\eta \sim 0.5$ condition (see Figures 3−5). Ideally, one would hope that the $I-V$ curves would be perfectly symmetric, but experimental factors such as the difference in materials of tip and substrate and the inherent asymmetry of the SAMs produces discernible $I-V$ asymmetries. Lowering the tip bias below V_{min} increased the noise of the STM feedback voltage required to maintain set point conditions, indicating that the tip was perturbing the electronic states of the monolayer.[47]

The $I-V$ data obtained from SAMs of DDT, ODT, and RC10TS exhibit significant differences in both their conductance gaps and their relative conductances at a given voltage bias. The conductance gap of the SAMs, i.e., the voltage range for which tunnel current is below the noise level of the instrument (1 pA), can be determined straightforwardly from the dI/dV data taken at V_{min} by extrapolating the slopes of the curves at high voltage bias toward zero current. For DDT, we estimate this to be 1.5 ± 0.5 V (see Figure 3). The E_f − HOMO energy level difference,[28−30] which is one-fourth of the conductance gap when $\eta = 0.5$, is 0.4 ± 0.2 eV. The $I-V$ curves and conductance spectra of ODT and RC10TS are similar to those of DDT but lose their symmetry more rapidly at higher set voltages (see

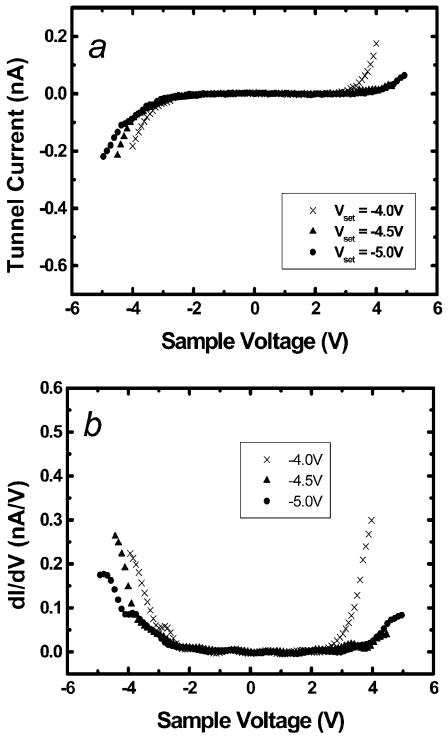

Figure 5. (a) $I-V$ data for RC10TS for a series of set voltages and a set current of 0.2 nA. (b) dI/dV data for RC10TS for a series of negative set voltages and a set current of 0.2 nA. The most symmetric dI/dV data are observed at a set voltage of -4.0 ± 0.2 V.

TABLE 1: Summary of Values Derived from STS Measurements under $\eta \sim 0.5$ Conditions

SAM	conduction gap (V)	$E_f - E_{Homo}$ (eV)	$(I/V)/G_o\|_{V=-1.5V}$	$V/I\|_{V=-1.5V}$ (Ω)
DDT	1.5 ± 0.5	0.4 ± 0.2	$(7.8 \pm 2.6) \times 10^{-7}$	$\sim 1.6 \times 10^{10}$
ODT	4.0 ± 0.5	1.0 ± 0.2	$(4.1 \pm 2.2) \times 10^{-8}$	$\sim 3.2 \times 10^{11}$
RC10TS	5.5 ± 0.5	1.4 ± 0.2	$(1.0 \pm 0.5) \times 10^{-8}$	$\sim 1.3 \times 10^{12}$

Figures 4 and 5). The estimated conductance gaps for these more insulating SAMs are 4.0 ± 0.5 and 5.5 ± 0.5 V, respectively, the latter being nearly four times larger than that of DDT (see Table 1). Effects, if any, from different end groups in the SAMs are expected to be minor relative to the tip's position above the substrate and are accommodated by adjusting the degree of overlap between electronic states in the molecule and the tip.

$|I/V|$ values for all three SAMs were evaluated at the V_{min} of DDT (-1.5 V) to provide meaningful comparisons of their relative conductances. In principle, molecular conductance values should be estimated at zero bias and expressed simply as $|dI/dV|_{V=0}$.[30] However, tunneling currents across these insulating SAMs at low bias are well below the noise levels of our instrument ($\sim$1 pA), preventing their straightforward measurements. As an alternative, we have determined relative conductances of the SAMs at the lowest voltage bias that would allow for a direct comparison, using $I-V$ data acquired at their respective V_{min}. $|I/V|$ values were normalized by $G_o = 2e^2/h$, the quantum of conductance. Thus, the conductances of DDT, ODT, and RC10TS at -1.5 V were estimated to be $7.8 \times 10^{-7} G_o$, $4.1 \times 10^{-8} G_o$, and $1.0 \times 10^{-8} G_o$, respectively (see Table 1).[48] These conductances are at least several orders of magnitude lower than those of relatively conductive molecules on Au such as xylenedithiol or the oligophenylenedithiols, whose transmission functions have been determined theoretically and in some cases experimentally.[10,26,36] In the case of DDT, our results compare favorably to those recently reported for decanethiol on Au using conductive AFM techniques.[16]

We observe a 20-fold difference in $|I/V|_{V=-1.5V}$ for DDT and ODT SAMs, which have equivalent chemisorptive properties but different thicknesses ($\sim$1.4 and 2.0 nm, respectively). This is less than expected for alkanethiol SAMs on Au with a 50% difference in chain length, whose low-bias conductances have been shown to be exponentially dependent with a decay constant of 1.1$-$1.2 Å^{-1}.[15,31,33] The simple reason for this discrepancy is that strong electric fields introduce significant nonlinearities into the $I-V$ relationship, which limits our ability to extrapolate these measurements to zero-bias conductances. However, such extrapolations may be of limited consequence for applications in which electrical insulation is a critical property.

We also observe a 4-fold difference in conductance for ODT and RC10TS SAMs, which have comparable thicknesses but different chemisorptive properties. The RC10TS SAM has a lower conductivity despite being bonded to the substrate by multiple gold$-$sulfur interactions per molecule. One significant factor is the strength of chemical bonding to the Au(111) surface: individual gold$-$sulfide ($Au-SR_2$) interactions are substantially weaker than gold$-$thiolate (Au$-$SR) interactions, implying that the electronic energy levels of the sulfide are less polarized by adsorption. A careful examination of various organosulfur adsorbates on Au(111) by X-ray photoelectron spectroscopy (XPS) demonstrated that the S(2p) binding energies of sulfides are hardly affected by adsorption onto gold, whereas those of thiols and disulfides are shifted by 1 eV or more upon binding.[49] Therefore, the sulfur atoms of alkanethiols provide relatively good electrical transmission to the Au atoms on the substrate surface, whereas the weak electronic coupling of the sulfide orbitals of RC10TS with the metal surface correlates with lower conductivity. Other theoretical studies on electronic transmission across SAMs have reached similar conclusions.[37,41]

The relatively high voltages and currents used to perform the STS measurements raise some other practical issues that must be addressed. One concern with the experimental conditions reported here is that a strong electric field can polarize molecular orbitals, effectively decreasing η below 0.5 at the threshold voltage bias.[28] Previous STM studies[17$-$25,27] of molecules adsorbed onto Au substrates have employed relatively small tunnel currents (3$-$30 pA) with subsequently low voltage requirements ($|V_{bias}| < 1.2$ V). However, the molecules in this study have relatively low polarizabilities because of their high volume fraction of saturated hydrocarbon so their electronic structures should not be strongly perturbed at high fields, although they may induce some nonlinearities (see above). Another concern is the possibility for oxidative damage or field-induced breakdown of the sample at high voltages. It has been shown that application of voltage bias in excess of 3 V on thiol-passivated Au surfaces can create etch pits and oxidize thiols under humid ambient conditions.[50,51] However, voltage-induced degradation has not been observed during tunneling in dry nitrogen and is thus unlikely to be an issue for tunneling experiments performed under UHV conditions. This is confirmed by the reproducibility of the STS studies: multiple $I-V$ measurements were taken repeatedly over the same spot at fields in excess of 1×10^9 V/m, but no discernible changes in data quality were observed.

There is general agreement that electron tunneling across SAMs on Au is mediated through-bond by a discrete number of molecules, whose local density of states offer the most efficient electronic path between tip and substrate. The conductance spectra presented in this study are also presumed to be representative of tunneling through a very limited number of molecules, because the lateral tip drift is less than one molecular cross section (0.2$-$0.6 nm) within the time scale of the STS measurements. Earlier calculations of tunneling probability as a function of SAM structure suggest that molecular orientation has only a modest effect on conductance, provided that conformational distortion is minimal.[33] In the case of alkanethiols such as DDT and ODT, molecules in well-ordered SAMs adopt an all-trans configuration with an orientation close to 30° from the surface normal.[52] In the case of RC10TS, evidence provided by Reinhoudt and co-workers suggest a nearly normal orientation to the Au(111) surface.[44]

On the basis of these assumptions, we can estimate the leakage current density through insulating SAMs on Au(111) to the first degree of approximation and compare them to theoretical estimates of the leakage current through thin SiO_2 layers on Si.[8] The molecular leakage current density $J(V)$ through a SAM can be expressed as

$$J(V) \cong VG(V)/(\pi r^2) \tag{5}$$

where $G(V)$ is represented by the conductance spectra at $\eta \sim 0.5$ and πr^2 is the approximate cross-sectional area of a molecule conducting the flow of electrons. The latter parameter can be derived from the molecular periodicities of the SAMs; we infer from previous structural studies that $r_{DDT} = 0.21$ nm and $r_{RC10TS} = 0.6$ nm.[25,52,53] A semilogarithmic $J-V$ plot for the 1.4-nm DDT SAM and the 2.0-nm RC10TS SAM reveals the superior insulating properties of the latter at high voltages (see Figure 6). SiO_2 layers with comparable leakage current densities were calculated to have thicknesses of 1.0 and 1.5 nm, respectively.[8] Although this comparison is semiquantitative at

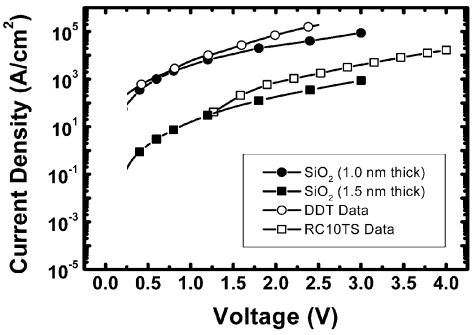

Figure 6. *J*−*V* plots comparing voltage-dependent leakage current through DDT on Au and RC10TS on Au with 1.0 and 1.5 nm SiO_2 layers on Si, as calculated in ref 8.

best, it strongly suggests that organic SAMs indeed have the potential to provide the necessary insulation for the efficient operation of molecular or nanoscale electronic circuits.

Conclusions

STS spectra obtained under $\eta \sim 0.5$ conditions can provide useful estimates of conductance for highly insulative SAMs on Au(111). The $\eta \sim 0.5$ criterion can be determined experimentally and independently of tip−sample distances or monolayer thicknesses. SAMs with different thicknesses and chemical bonding on Au exhibit large differences in both their conductance gaps and their conductances at high voltage bias. The RC10TS SAM was shown to have exceptional electrical insulation properties, comparable to that of a 1.5-nm layer of SiO_2 on Si. High-quality SAMs may thus possess sufficient electrical insulation to be used in future device applications.

Acknowledgment. We thank Ronald P. Andres, Supriyo Datta, and Clifford P. Kubiak for helpful conversations throughout the course of this work. R.R. thanks Julio Gomez and Oscar Custance at the Laboratorio de Nuevas Microscopias at the Universidad Autonoma de Madrid for their continued help and support. We gratefully acknowledge financial support from the National Science Foundation (9708107-DMR) and the Integrated Detection of Hazardous Materials program managed by the Center for Sensing Science and Technology (Purdue University) and NSWC (Crane, Indiana).

References and Notes

(1) Andres, R. P.; Datta, S.; Janes, D. B.; Kubiak, C. P.; Reifenberger, R. In *Handbook of Nanostructured Materials and Nanotechnology*, Vol. 3; Nalwa, H. S., Ed.; Academic Press: New York, 2000; pp 179−231.
(2) Everhart, D. S. *Chemtech* **1999**, *29*, 30−37.
(3) Lee, T.; Liu, J.; Janes, D. B.; Kolagunta, V. R.; Dicke, J.; Andres, R. P.; Lauterbach, J.; Melloch, M. R.; McInturff, D.; Woodall, J. M.; Reifenberger, R. *Appl. Phys. Lett.* **1999**, *74*, 2869−2871.
(4) Metzger, R. M. *Acc. Chem. Res.* **1999**, *32*, 950−957.
(5) Chen, J.; Reed, M. A.; Rawlett, A. M.; Tour, J. M. *Science* **1999**, *286*, 1550−1552.
(6) Reed, M. A.; Zhou, C.; Muller, C. J.; Burgin, T. P.; Tour, J. M. *Science* **1997**, *278*, 252−254.
(7) Buchanan, D. A. *IBM J. Res. Dev.* **1999**, *43*, 245−264.
(8) Lo, S.-H.; Buchanan, D. A.; Taur, Y. *IBM J. Res. Dev.* **1999**, *43*, 327−337.
(9) Muller, D. A.; Sorsch, T.; Moccio, S.; Baumann, F. H.; Evans-Lutterodt, K.; Timp, G. *Nature* **1999**, *399*, 758−761.
(10) Andres, R. P.; Bein, T.; Dorogi, M.; Feng, S.; Henderson, J. I.; Kubiak, C. P.; Mahoney, W.; Osifchin, R. G.; Reifenberger, R. *Science* **1996**, *272*, 1323−1325.
(11) Li, T. T.-T.; Weaver, M. J. *J. Am. Chem. Soc.* **1984**, *106*, 6107−6108.
(12) Porter, M. D.; Bright, T. B.; Allara, D. L.; Chidsey, C. E. D. *J. Am. Chem. Soc.* **1987**, *109*, 3559−3568.
(13) Sachs, S. B.; Dudek, S. P.; Hsung, R. P.; Sita, L. R.; Smalley, J. F.; Newton, M. D.; Feldberg, S. W.; Chidsey, C. E. D. *J. Am. Chem. Soc.* **1997**, *119*, 10563−10564.
(14) Smalley, J. F.; Feldberg, S. W.; Chidsey, C. E. D.; Linford, M. R.; Newton, M. D.; Liu, Y.-P. *J. Phys. Chem.* **1995**, *99*, 13141−13149.
(15) Wold, D. J.; Frisbie, C. D. *J. Am. Chem. Soc.* **2001**, *123*, 5549−5556 and references therein.
(16) Cui, X. D.; Primak, A.; Zarate, X.; Tomfohr, J.; Sankey, O. F.; Moore, A. L.; Moore, T. A.; Gust, D.; Harris, G.; Lindsay, S. M. *Science* **2001**, *294*, 571−574.
(17) Anselmetti, D.; Baratoff, A.; Güntherodt, H.-J.; Delamarche, E.; Michel, B.; Gerber, Ch.; Kang, H.; Wolf, H.; Ringsdorf, H. *Europhys. Lett.* **1994**, *27*, 365−370.
(18) Delamarche, E.; Michel, B.; Gerber, Ch.; Anselmetti, D.; Güntherodt, H.-J.; Wolf, H.; Ringsdorf, H. *Langmuir* **1994**, *10*, 2869−2871.
(19) Delamarche, E.; Michel, B.; Kang, H.; Gerber, Ch. *Langmuir* **1994**, *10*, 4103−4108.
(20) Poirier, G. E.; Tarlov, M. J. *Langmuir* **1994**, *10*, 2853−2856.
(21) Poirier, G. E.; Tarlov, M. J.; Rushmeier, H. E. *Langmuir* **1994**, *10*, 3383−3386.
(22) Schönenberger, C.; Jorritsma, J.; Sondag-Huethorst, J. A. M.; Fokkink, L. G. J. *J. Phys. Chem.* **1995**, *99*, 3259−3271.
(23) Kang, J.; Rowntree, P. A. *Langmuir* **1996**, *12*, 2813−2819.
(24) Bumm, L. A.; Arnold, J. J.; Charles, L. F.; Dunbar, T. D.; Allara, D. L.; Weiss, P. S. *J. Am. Chem. Soc.* **1999**, *121*, 8017−8021.
(25) Raible, S.; Pfeiffer, J.; Weiss, T.; Clauss, W.; Goepel, W.; Schurig, V.; Kern, D. P. *Appl. Phys. A* **2000**, *70*, 607−611.
(26) Dorogi, M.; Gomez, J.; Osifchin, R.; Andres, R. P.; Reifenberger, R. *Phys. Rev. B* **1995**, *52*, 9071−9077.
(27) Bumm, L. A.; Arnold, J. J.; Cygan, M. T.; Dunbar, T. D.; Burgin, T. P.; Jones, L., II.; Allara, D. L.; Tour, J. M.; Weiss, P. S. *Science* **1996**, *271*, 1705−1707.
(28) Datta, S.; Tian, W.; Hong, S.; Reifenberger, R.; Henderson, J. I.; Kubiak, C. P. *Phys. Rev. Lett.* **1997**, *79*, 2530−2533.
(29) Tian, W.; Datta, S.; Hong, S.; Reifenberger, R. G.; Henderson, J. I.; Kubiak, C. P. *Physica E* **1997**, *1*, 304−309.
(30) Tian, W.; Datta, S.; Hong, S.; Reifenberger, R.; Henderson, J. I.; Kubiak, C. P. *J. Chem. Phys.* **1998**, *109*, 2874−2882.
(31) Bumm, L. A.; Arnold, J. J.; Dunbar, T. D.; Allara, D. L.; Weiss, P. S. *J. Phys. Chem. B* **1999**, *103*, 8122−8127.
(32) Hong, S.; Reifenberger, R.; Tian, W.; Datta, S.; Henderson, J. I.; Kubiak, C. P. *Super. Microsc.* **2000**, *28*, 289−303.
(33) Salmeron, M.; Neubauer, G.; Folch, A.; Tomitori, M.; Ogletree, D. F.; Sautet, P. *Langmuir* **1993**, *9*, 3600−3611.
(34) Samanta, M. P.; Tian, W.; Datta, S.; Henderson, J. I.; Kubiak, C. P. *Phys. Rev. B* **1996**, *53*, R7626−R7629.
(35) Widrig, C. A.; Alves, C. A.; Porter, M. D. *J. Am. Chem. Soc.* **1991**, *113*, 2805−2810.
(36) Datta, S. *Electronic Transport in Mesoscopic Systems*; Cambridge University Press: Cambridge, U.K., 1995.
(37) Joachim, C.; Vinuesa, J. F. *Europhys. Lett.* **1996**. *33*, 635−640.
(38) Mujica, V.; Kemp, M.; Roitberg, A.; Ratner, M. *J. Chem. Phys.* **1996**, *104*, 7296−7305.
(39) Hsu, C.-P.; Marcus, R. A. *J. Chem. Phys.* **1997**, *106*, 584−598.
(40) Emberly, E.; Kirczenow, G. *Nanotechnology* **1999**, *10*, 285−289.
(41) Magoga, M.; Joachim, C. *Phys. Rev. B* **1997**, *56*, 4722−4729.
(42) Thoden van Velzen, E. U.; Engbersen, J. F. J.; Reinhoudt, D. N. *Synthesis* **1995**, 989−997.
(43) Thoden van Velzen, E. U.; Engbersen, J. F. J.; Reinhoudt, D. N. *J. Am. Chem. Soc.* **1994**, *116*, 3597−3598.
(44) Thoden van Velzen, E. U.; Engbersen, J. F. J.; de Lange, P. J.; Mahy, J. W. G.; Reinhoudt, D. N. *J. Am. Chem. Soc.* **1995**, *117*, 6853−6862.
(45) Chidsey, C. E. D.; Bertozzi, C. R.; Putvinski, T. M.; Mujsce, A. M. *J. Am. Chem. Soc.* **1990**, *112*, 4301−4306.
(46) Bain, C. D.; Troughton, E. B.; Tao, Y.-T.; Evall, J.; Whitesides, G. M.; Nuzzo, R. G. *J. Am. Chem. Soc.* **1989**, *111*, 321−335.
(47) At this time, it is an unsettled question whether the tip actually becomes embedded in the SAM or whether the electric field between the tip and upper surface of the SAM becomes so great as to produce instability in the tunneling current.
(48) For our experimental conditions, the minimal measurable conductance unit is $1 \times 10^{-8} G_o$.
(49) Zhong, C.-J.; Brush, R. C.; Anderegg, J.; Porter. M. D. *Langmuir* **1999**, *15*, 518−525.
(50) Kim, Y.-T.; Bard, A. J. *Langmuir* **1992**, *8*, 1096−1102.
(51) Schoer, J. K.; Zamborini, F. P.; Crooks, R. M. *J. Phys. Chem. B* **1996**, *100*, 11086−11091.
(52) Dubois, L. H.; Nuzzo, R. G. *Annu. Rev. Phys. Chem.* **1992**, *43*, 437−463.
(53) Schönherr, H.; Vancso, G. J.; Huisman, B.-H.; van Veggel, F. C. J. M.; Reinhoudt, D. N. *Langmuir* **1997**, *13*, 1567−1570.